Electronic Supplementary Material (ESI) for Green Chemistry.
This journal is © The Royal Society of Chemistry 2015

Use of ultrasonic cavitation for near surface structuring of robust and low-cost AlNi catalysts for hydrogen production

*P. V. Cherepanov[a], I. Melnyk[a], E. V. Skorb[b], P. Fratzl[b], E. Zolotoyabko[c], N. Dubrovinskaia[d], L. Dubrovinsky[e], Y. S. Avadhut[f], J. Senker[f], L. Leppert[g], S. Kümmel[g], and D. V. Andreeva[a]**

I. Aluminum-Nickel binary phase diagram

Fig. S1 shows the aluminum-nickel binary phase diagram (Al-Ni BPD). The used composition is 50:50 wt. % (shown by the gray line).

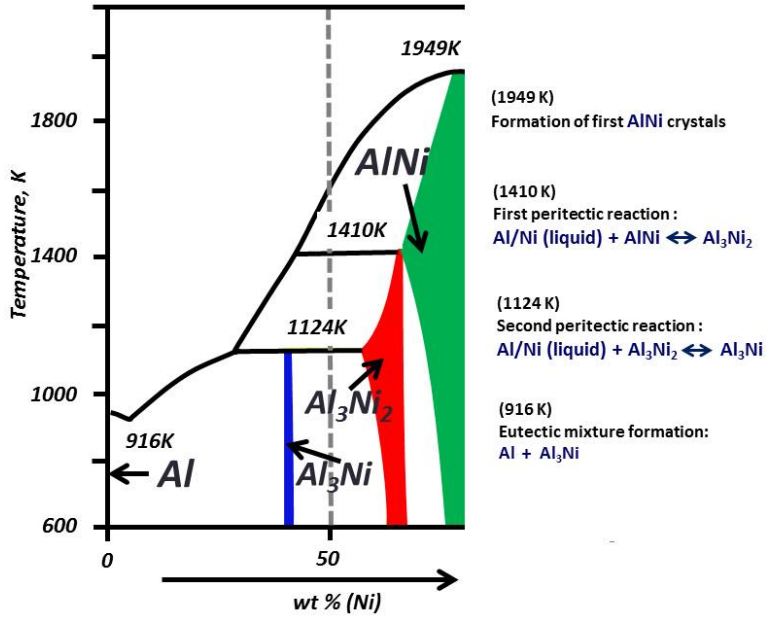

Fig. S1 Aluminum-nickel binary phase diagram (Ni weight percent ranging from 0 to about 70 wt.%) adopted from Ref.[1]

II. Sample preparation

Preparation of metal alloys

Before melting, aluminum and nickel foils (1.0 mm thick, 99.999% trace metals basis, Aldrich, Germany) of required weight were folded together and pressed into a rectangle-shaped pellet. Upon cooling of the melt, newly prepared alloy was pressed into a plate and folded back to the rectangular shape followed by re-melting. The entire procedure was repeated four times to ensure that aluminum and nickel have been completely mixed. Melting and cooling steps in alloy preparation were performed in argon atmosphere to prevent oxidation. The final alloy

plate was processed in the milling machine (Rotormühle Fritsch Pulverisette 14) and meshed towards obtaining an alloy powder with an average particle size of ~140 μm. The pure intermetallic phases, Al_3Ni_2 and Al_3Ni (~150 μm), have been supplied by Goodfellow GmbH (Germany). The powder X-ray diffractions (PXRD) of the pure phases are shown in **Fig. S2**.

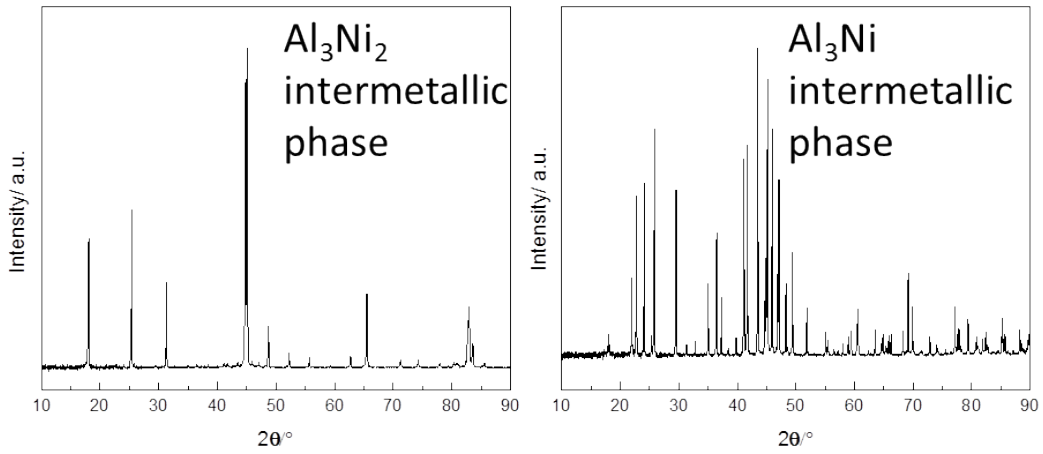

Fig.S2 PXRD patterns of the pure phases.

High Power Ultrasound (HPUS) treatment of metal alloys

The sonication cell is shown in **Fig. S3**.

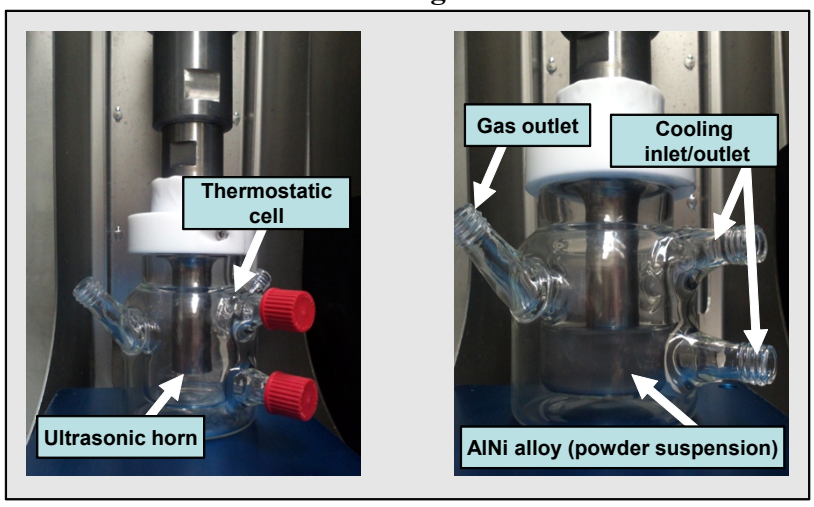

Fig. S3 Photo of the cell for HPUS treatment of the AlNi powdered alloys.

AlNi powder (4g) was dispersed in 40 mL ethanol and sonicated for 60 min with a Hielscher UIP1000hd, (Hielscher Ultrasonics GmbH, Germany) operated at 20 kHz with a maximum output power of 1000 W. The apparatus is equipped with an ultrasonic horn BS2d22 (head

area of 3.8 cm^2) and a booster B2-1.8. The maximum intensity was calculated to be 140 W cm^{-2} at mechanical amplitude of 140 μm. To avoid overheating during sonication the experiment was carried out in a homemade thermostatic cell connected to a thermostat (Huber GmbH, Germany). The temperature was monitored during the treatment and kept at 298 K. After the HPUS treatment, the metal particles were separated from the supernatant by centrifugation at a speed of 10 000 rpm for 1h and washed with absolute ethanol followed by drying in vacuum at room temperature.[2]

I. Sample characterization

Electrochemical characterization

For electrochemical measurements a three-electrode cell consisting of Ag/AgCl/ (saturated KCl) reference electrode (potential was converted to standard hydrogen electrode (SHE)), the Pt foil (6 cm^2) counter electrode, and paraffin impregnated graphite electrode (PIGE) as a working electrode was employed. HIUS modified AlNi alloy particles were immobilized on PIGE with use of Nafion as a binder solution. Linear Sweep Voltammetry (LSV) measurements were performed on a 510 V10 Potentiostat/Galvanostat (MaterialMates, Italy) in the potential region -0.2V to-0.9V with a scan rate of 50mV/s and use of 1M H_2SO_4 as a supporting electrolyte.

To determine lifetime performance of the ultrasonically treated catalyst for HER, galvanostatic responses were recorded at 60 mA/cm^2 for 9 consecutive hours.

^{27}Al Magic Angle Spinning Nuclear Magnetic Resonance (MAS NMR)

The solid state ^{27}Al NMR spectra were recorded on a Bruker AvanceII 300 tuned to a resonance frequency of 78.2 (7.04 T). All magic angle spinning (MAS) NMR experiments were carried out with a commercial 2.5 mm triple resonance MAS probe operating with spinning speed of 20 kHz. The chemical shifts are reported with respect to a solution of $AlCl_3$ adjusted to a pH of 1 with HCl (δ_{iso} = 0 ppm). All spectra were acquired using a single pulse excitation with a pulse length of 1.5 μs and a recycle delay of 0.2 s. To assure a selective excitation of the central transition, the corresponding nutation frequency was adjusted to 16.7 kHz based on the $AlCl_3$ reference solution.

^{27}Al MAS NMR spectroscopy was used to identify the individual intermetallic phases near the surfaces of the AlNi nanoparticles. The sensitivity towards the surfaces arises from the

skin effect.[3] It describes the ability of the radio-frequency (rf) field to penetrate into conducting and magnetic material, respectively. The skin depth, *d*, is proportional to $\nu_0^{-1/2}$, $\mu_r^{-1/2}$ and $\rho^{1/2}$ with ν_0 being the Lamor frequency, μ_r being the relative permeability and ρ being the electric resistance. While ν_0 is constant for all experiments, ρ and μ_r might vary for the individual Al_xNi_y phases studied here. In particular, μ_r is 2-3orders of magnitude higher for ferromagnetic materials, as compared to Pauli paramagnets, such as metallic aluminum. However, due to the gradual changes observed for the pristine and sonicated materials no strong influence on the skin depth is expected rendering ^{27}Al NMR into a semi-quantitative technique in this case. Thus a tentative interpretation of the spectral intensities in terms of phase composition should be possible.

While metallic Al depicts a sharp resonance at 1640 ppm, Al_3Ni is characterized by two broad peaks at 940 ppm and 640 ppm with an intensity ratio of 1:2. Al_3Ni_2 exhibits single resonance at 340 ppm. All three resonances depict a line shape typical for a second order quadrupolar broadening (**Fig. 4e, f**). The experimental ^{27}Al isotropic chemical shift (δ_{iso}), nuclear quadrupole coupling constants (C_q), anisotropy (η_q), and the individual contributions from each AlNi phases in atomic percentage are tabulated in the **Table S1**.

Table. S1: ^{27}Al NMR chemical shift, nuclear quadrupole coupling constants (C_q), anisotropy (η_q) and the individual contributions (at%) from each phase of AlNi alloy.

AlNi(50/50)	Parameters	Metallic Al	Al_3Ni-site 1	Al_3Ni-site 2	Al_3Ni_2	$Al(OH)_3$
	δ_{iso} / ppm	1638.0	940.0	641.0	340.0	0.0
Initial	C_q / kHz	--	9151.73	9026.70	8822.00	--
	η_q	--	0.55	0.59	0.67	--
	at%	26.23%	13.9%	32.94%	25.65%	1.23%
Sonicated	C_q / kHz	--	9787.72	8948.54	8956.11	--
	η_q	--	0.57	0.60	0.69	--
	at%	27.01%	15.57%	29.01%	27.05%	1.37%

Electron microscopy

Transmission electron microscopy (TEM) and selected area electron diffractions (SAED) were performed with a LEO 922 EFTEM instrument operating at 200 kV.

Scanning electron microscopy (SEM) and energy dispersive X-ray spectroscopy (EDS) measurements were carried outwith a Gemini Leo 1550 instrument at an operating voltage of

3keV. The results of surface chemical analysis for the pristine AlNi alloy (50 wt.% of Ni) are shown in **Table S2**.

Table S2. EDS analysis of the surface of the initial AlNi (50 wt.% Ni) particles.

Elements, atom.%	Al	Ni	Al:Ni
Analyzed area 1	21.40	28.10	1:1.3
Analyzed area 2	32.70	22.87	3:2
Analyzed area 3	28.75	44.65	2:3

Powder X-ray-diffraction

Powder X-ray diffraction (PXRD) measurements with intermetallic samples were carried out by the aid of a Stoe STADI P X-ray transmission diffractometer, equipped with a Cu sealed tube and built-in Ni filter (Cu Kα radiation, λ = 1.54056 Å). The phase composition was estimated using Rietvild refinement.

The PXRD profiles, as functions of double Btagg angle, 2θ, are shown in **Fig. S4**. For extracting important crystallographic information, i.e. crystallite size, D, and average microstrain fluctuations, ε,we used the standard Williamson – Hall (W-H) approach.[4-6]

In the W-H method, the measured widths, β_{hkl}, of diffraction peaks with Miller indices, *hkl*, (after applying instrumental correction), are presented in the following form:

$$\beta_{hkl}cos\theta = \left(\frac{k\lambda}{D}\right) + (4\varepsilon sin\theta)$$

where shape factor k = 0.94. It is worth to mention that only non-overlapping diffraction peaks were used by us for this analysis. The classical W-H equation assumes that the microstrain fluctuations, ε, are independent of crystallographic direction.

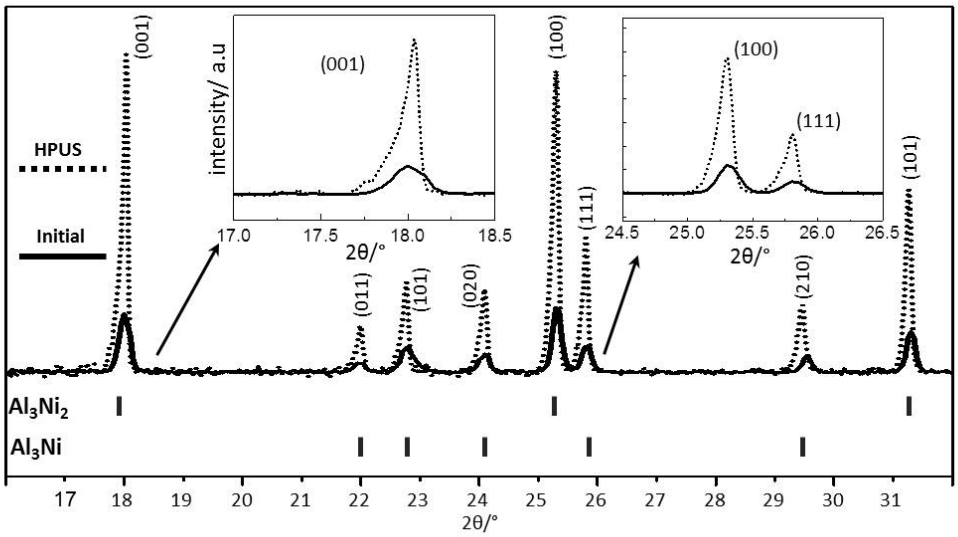

Fig. S4 Powder X-ray diffraction patterns of the initial (solid line) and ultrasonically modified (dashed line) AlNi ($Ni_{50\ wt.\%}$) with evidence for peak narrowing (insets).

The temperature effect on crystal size of the intermetallics in AlNi particles

Fig. S5 shows the dependence of the crystal sizes of Al_3Ni_2 and Al_3Ni phases in the samples that were heated in oven for 1 h at different temperatures. We see that up to 700°C the size of the crystals strongly depends on the applied temperature, while above this temperature some kind of saturation is reached. Placing the crystal size of the sonicated samples on this plot, we can estimate the effective temperature that is achieved within metal particles upon HPUS. Thus estimated average effective temperature in the sonicated particles was found to be about ~550°C (823 K).

As is seen in the right-hand panel in Figure S5, above 800°C (1073 K) the Al_3Ni phase is disappeared, i.e. is transformed into the Al_3Ni_2 phase. Thus, ultrasonication is able to selectively convert the catalytically ineffective Al_3Ni phase into beneficial Al_3Ni_2 phase in the interfacial region of the AlNi particles.

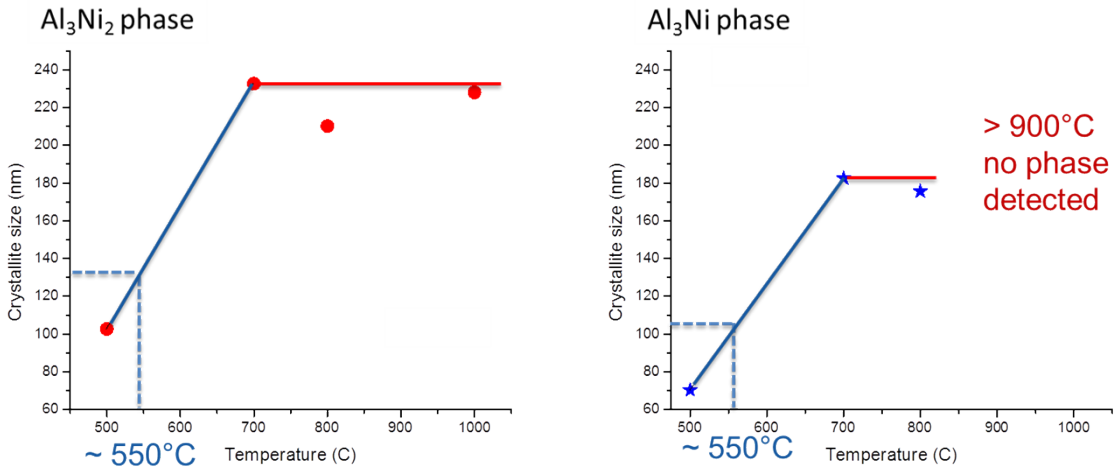

Fig. S5 Crystal size vs. particle temperature: the samples were heated at selected temperatures for 1h. Duration of the heat treatment in the oven is equal to that for the particle treatment by HPUS. The crystal sizes for Al_3Ni_2 and Al_3Ni phases, indicated by dashed lines, correspond to those measured by PXRD in the HPUS treated samples.

DFT Calculations

We performed density functional theory calculations using the Vienna ab-initio Simulation Package (VASP).[7] Ionic cores were described within the projector augmented waves formalism.[8] As we want to compare our free energies of hydrogen adsorption to literature values we used a similar setup and computational parameters as in Ref.[9, 10] With this we obtain a free energy of -0.08 eV for hydrogen adsorption on Pt(111) which agrees with the literature value[9] within 0.01 eV. We used a kinetic energy cutoff of 400 eV and 4x4x1 Monkhorst-Pack k-point meshes[11] in all calculations. Hydrogen adsorption energies were calculated using a periodically repeated surface slab model. To minimize spurious interactions, the vacuum region between neighboring supercells was chosen to be 20 Å. Additionally, dipole corrections were used. All energies were calculated self-consistently using the RPBE exchange-correlation functional.[12] We tested all possible hydrogen adsorption positions both on the $Al_3Ni(010)$ surface (both sides of the slab are equivalent) and on both sides of the $Al_3Ni_2(100)$ surface. A local geometry optimization was performed in all cases. Optimizations were considered as converged when the forces on all atoms were smaller than 0.02 eV/Å. For both compounds the surface cell was repeated twice in the directions parallel to the surface and three times in the direction normal to the surface. In each case, the positions of the atoms in the bottom two surface layers were kept fixed while the top layer was allowed to relax. We checked that letting the top two layers relax changes the hydrogen adsorption energy by less than 0.01 eV. The hydrogen adsorption energy was calculated as $\Delta E_H = E(surf+H) - E(surf) - 1/2E(H_2)$. For both compounds the energetically most favorable

hydrogen position is on top of the highest lying Al atom of the surface cell. To obtain the free energy diagram shown in Fig. 1, we followed Ref.[8] and calculated the free energy of the adsorbed state as $\Delta G_{H*} = \Delta E_H + \Delta E_{ZPE} - T\,\Delta S_H$, where ΔE_{ZPE} is the difference of zero point energies between the adsorbed state and the gas phase state. The vibrational entropy of the adsorbed state is considered small so that $\Delta S_H \cong -0.5 \cdot S^0_{H_2}$, which is the entropy of H_2 in the gas phase at standard conditions (see Ref.[9] and references therein). The vibrational frequencies of H adsorbed on Al_3Ni_2 are 1816 cm^{-1}, 454 cm^{-1} and 367 cm^{-1}, which leads to a ΔE_{ZPE} of 0.03 eV and thus $\Delta G_{H*} = \Delta E_H + 0.23$ eV. This value is also taken for hydrogen adsorption on Al_3Ni.[9,10]

We also looked at Al_3Ni_2 (001) in our calculations and tested several different adsorption positions on both "sides" of an Al_3Ni_2(001) surface slab. Similar to the (100) surface, the top and bottom of the surface slab look differently. The energetically most favourable position for hydrogen adsorption is a hollow site on the Al-rich side of the slab. The corresponding free energy is -0.30eV. The free energies of all other adsorption positions that we tested (on top of Ni and Al atoms) are also far away from zero. Thus, the simulations rule out (001) as the active phase.

References

1. D. Batalu, G. Cosmeliata, A. Aloman, *Metalurgia Inter.* 2006, **11**, 36.
2. J. Dulle, S. Nemeth, E. V. Skorb, T. Irrgang, J. Senker, R. Kempe, A. Fery, D. V. Andreeva, *Adv. Func. Mater.* 2012, **22**, 3128.
3. R. Bhattacharyya, B. Key, H. Chen, A. S. Best, A. F. Hollenkamp, C. P. Grey, *Nat. Mater*. 2010, **9**, 504.
4. T. Ungar, A. Revesz, A. Borbely, *J. Appl. Crystallogr*. 1998, **31**, 554.
5. K. Venkateswarlu, A. C. Bose, N. Rameshbabu, *Physica* 2010, **B405**, 4256.
6. A. K. Zak, W. H. A. Majid, M. E. Abrishami, R. Yousefi, *Solid State Sci*. 2011, **13**, 251.
7. (a) G. Kresse, J. Furthmüller, *Comput. Mater. Sci.***1990**, *6*, 15; (b) G. Kresse, J. Furthmüller, *Phys. Rev.* 1996, **B54**, 11169.
8. P. E. Blöchl, *Phys. Rev.* 1994, **B50**, 17953.
9. J. K. Nørskov, T. Bligaard, A. Logadottir, J. R. Kitchin, J. G. Chen, S. Pandelov, U. Stimming, *J. Electrochem. Soc.* 2005, **152**, J23.
10. B. Hinnemann, P. G. Moses, J. Bonde, K. P. Jorgensen, J. H. Nielsen, S. Horch, I. Chorkendorff, J. K. Nørskov, *J. Am. Chem. Soc.* 2005, **127**, 5308.
11. H. J. Monkhorst, J. D. Pack, *Phys. Rev.* 1976, **B13**, 5188.

12. B. Hammer, L. B. Hansen, J. K. Nørskov, *Phys. Rev.* 1999, **B46**, 7413.